EXPERIMENTAL EVALUATION OF EFFECT OF STOPPERS ON PERFORMANCE OF BUCKLING-RETRAINED BRACES

Chun-Lin WANG[1], Jyunki FUNAYAMA[2], Fumiaki IMASE[3], and Tsutomu USAMI[4]

[1] Post-doctoral researcher, Department of Civil Engineering, Meijo University
Tempaku-ku 1-501, Nagoya, Japan, wangmeijo@gmail.com
[2] Master student, Department of Civil Engineering, Meijo University
Tempaku-ku 1-501, Nagoya, Japan, 103437009@ccalumni.meijo-u.ac.jp
[3] Master student, Department of Civil Engineering, Meijo University
Tempaku-ku 1-501, Nagoya, Japan, 113437002@ccalumni.meijo-u.ac.jp
[4] Professor, Department of Civil Engineering, Meijo University
Tempaku-ku 1-501, Nagoya, Japan, usamit@meijo-u.ac.jp

Recently, series of low-cycle fatigue tests have been conducted to develop high-performance Buckling-Restrained Braces (BRBs) for improving the seismic performance of steel bridges. This paper presents studies on the influence of stoppers on the low-cycle fatigue performance of steel BRBs. These stoppers are used to prevent the relative movement between the brace member and restraining members. Results show that BRB's specimens with stoppers possess the better performance and the relatively larger safety margin than the specimens without stoppers. The cumulative inelastic deformation performance of steel BRBs without stoppers decreased by about 40% compared to BRBs with stoppers.

***Key words**: Steel Bridge, Buckling-restrained brace, Stopper, Low-cycle fatigue performance, Safety margin*

1. INTRODUCTION

In the last few decades, the recent trend of seismic design methodology for steel building structures is that the primary members of building structures almost remain elastic and most of the inelastic deformations are enforced to occur in some energy absorption members, such as bracing members. Residual deformation of structures after a severe earthquake could be reduced based on this design philosophy because most of main members have not been damaged during the earthquake excitation.

This design philosophy has been gradually implemented and refined in steel bridge structures. Developing a reliable method of designing the energy absorption equipment is indispensable. One way is to utilize some lateral or diagonal bracing members in a bridge structure as energy absorption members. Members in the lateral bracing system will be performed under cyclic compression and tension so that they should have high energy absorption capacity. Therefore, in order to obtain a stable performance, the global buckling of bracing members must be restrained by the restraining cover members. This is the buckling-restrained brace (BRB), which attracts more and more attentions because it does not buckle in compression but yield in both tension and compression and represents an effective energy absorption mechanism for damping of engineering structures with low cost.

As an axial-type hysteretic device, BRBs are widely studied on component behavior and system applications in building and bridge engineering. It has been indicated from recent researches conducted by authors[1, 2] that BRBs were employed to replace insufficient lateral braces and cross diagonal braces for retrofitting an existing steel arch bridge, which leads to damage concentration in sacrificing damping devices and mitigates the damage of main structures. Moreover, a displacement-controlled pseudo-static test[1] show that BRBs process excellent cumulative inelastic ductility capacity before the failure of the core brace member, far larger than the minimum required value of 200 (the ratio of the cumulative inelastic strain to the yield strain of the brace member) by AISC seismic provisions[3)].

2. HIGH-PERFORMANCE BRB

Based on authors' recent researches, a new concept of high-performance BRBs (HPBRBs) is proposed that no replacement of BRBs is needed during the 100-year lifecycle of bridges and BRBs are likely to endure three times of strong earthquakes without severe damage[4)]. Therefore, besides general performance requirements for BRBs used in building engineering as given in the reference[3)], additional special performance requirements for HPBRBs in bridge engineering are summarized as follows[4)]: (1) Stable hysteretic characteristics and high energy dissipation capacity; (2) High deformation capacity; (3) High low-cycle fatigue strength; (4) Easy fabrication and construction with low cost; (5) High durability; (6) No need of replacement.

In the performance-based seismic verification method, two performance indices, i.e., the axial deformation and the low-cycle fatigue performance, are often employed to quantify the performance demands required for BRBs[5)]. For the strong earthquakes (i.e., Level 2 earthquakes), the expressions of the BRB's capacity requirements are given as follows,

$$\gamma \cdot \varepsilon_{\max} \leq \varepsilon_u \tag{1}$$

$$CID = \gamma \cdot \sum_{i=1}^{n} \left| \varepsilon_{pi} \right| \leq CID_{\lim} \tag{2}$$

where ε_{max} = maximum axial strain demand of BRB; ε_u = ultimate axial strain capacity of BRB; *CID* = cumulative inelastic deformation demand; ε_{pi} = plastic component of axial strain of BRB, as shown in Figure 1; CID_{lim} = limit value of the *CID* capacity of BRB; γ = partial factor (=1.16). In JSCE Specifications[5)], a nonlinear time history analysis considering the material and geometrical nonlinearities is required to obtain demand values. According to our researches, authors[4)] have recommended that the target maximum deformation and cumulative inelastic deformation demands of BRBs should be over 3% (the safety factor is about 1.3) and 70% (about three times of the maximum *CID* value), respectively.

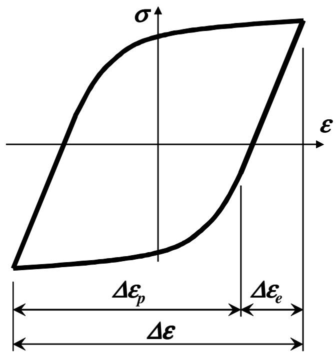

Figure 1. Stress-strain curve of BRB

3. INFLUENCE OF STOPPERS

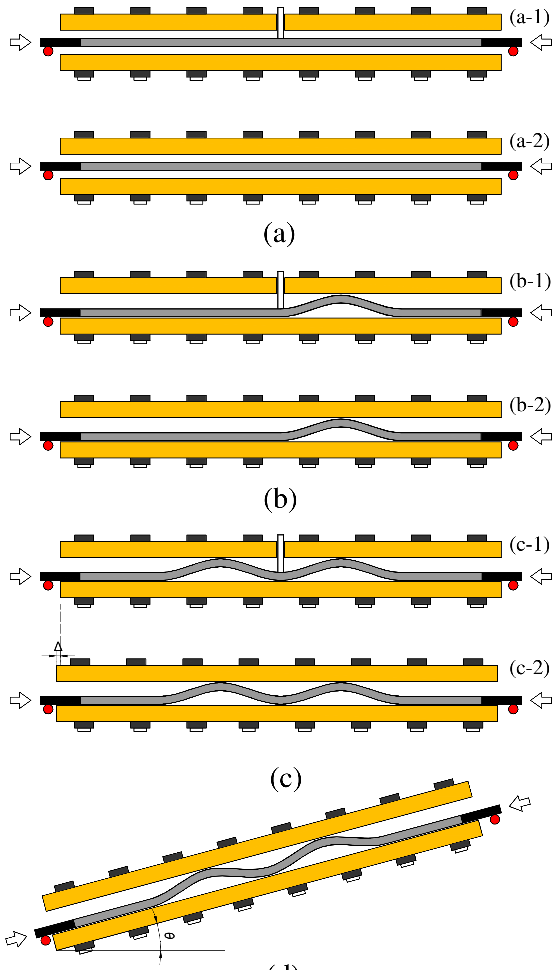

Figure 2. Influence of stoppers

In order to meet the performance demands of HPBRBs, series of low-cycle fatigue tests have been conducted to evaluate a new type of steel BRBs proposed by authors[6, 7)]. During these experiments, two steel pins were welded at the middle of the brace member and used to prevent the relative movement between the brace member and the restraining members, as shown in Figures 2 and 3. The BRB given in Figure 2 is a sketch of the BRB presented in Figure 3. Considering these pins are used to stop the movement of the restraining members, they are named stoppers in this paper and attracted our attentions. As shown in Figure 2(a), two BRBs with and without stoppers are given under the compression. With the compressive loading increasing, the restrained buckling of the brace member gradually takes place but the location of the buckling is random, as shown in Figure 2(b). Consequently, the frictional force takes place after the interaction between the restraining member and the brace member and drives the restraining members to move when this frictional force is enough large. As shown in Figure 2(c), restraining members of the BRB without stoppers are moved, which has been verified by the following experiments. Moreover, as shown in Figure 2(d), if a BRB is installed with an inclination, the driving force is composed of the frictional force and the weight of the restraining members. So, in order to avoid the influence of the weight of the restraining members, the testing specimens were horizontally placed.

In this paper, the influence of the stoppers on the low-cycle fatigue performance of the HPBRBs is first experimental discussed. Considering that the strain amplitude employed in this experiment is larger than the required axial strain of HPBRB, the stoppers actually affect the performance safety margin of HPBRB. Details of the experiment, including four steel specimens, are given as follows. All the tests were performed at the Advanced Research Center for Seismic Experiments and Computations (ARCSEC) at Meijo University.

3. TEST SPECIMENS AND PROGRAM

(1) BRB's configuration

As shown in Figure 3, the presented all-steel BRB mainly consist of a steel plate brace member (BM), a pair of restraining members (RMs) connected by high-strength bolts through two filler members, and unbonding material stuck to the brace member as the isolation material in order to reduce the friction between the BM and RMs. This unbonding material is a kind of the butyl rubber of 1 mm in thickness.

The nominal dimensions of the BM are given in Figure 4, while measured dimensions and structural properties are listed in Table 1. A flat steel plate is used as the BM, and cruciform sections at both ends are expanded by welding 12mm thick rib stiffeners to each side of the plate. It is helpful for preventing the out-of-plane buckling of the unrestrained segment of the BM. The BM is made of SM400A mild steel. Three JIS No.1-typed test pieces for each series are made from the same steel of the BM and average values tested as material constants are listed in Table 2, respectively. At the center of FE-4.0 and FT-3.5 specimens' BMs, two welded stoppers of 9 mm in diameter and 30 mm in height are used to prevent the relative movement between the BM and RMs in the longitudinal direction. But there is nothing at the center of FT-3.5(NS) and FT-4.0(NS) specimens.

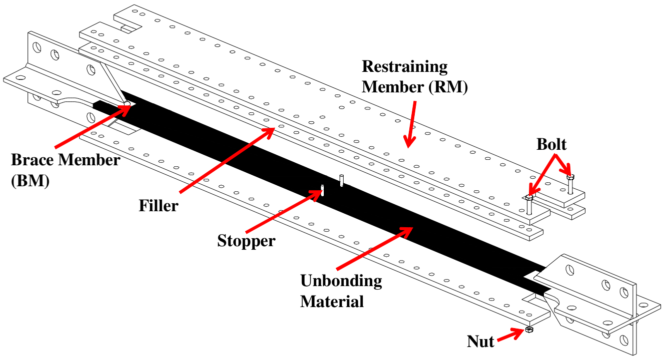

Figure 3. Assemblage of steel BRB

Figure 5 gives cross-sectional details of the BRB. The BM is sandwiched by a pair of RMs, and small gaps, d and d_0, are provided between the BM and RMs or filler members. Geometric dimensions and structural properties of RMs are listed in Table 3. The same SM400A mild steel is used for RMs and filler members made of flat steel plates. Nominal values of gap widths are given in Table 3, together with measured material properties of RMs.

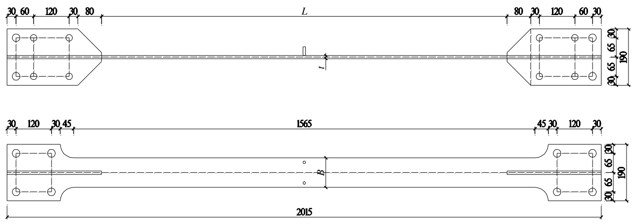

Figure 4. Dimensions of BM

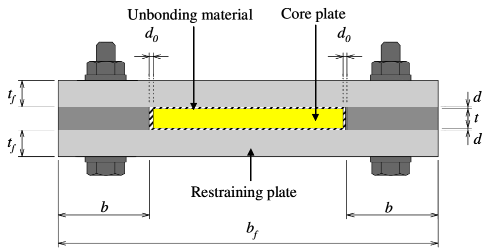

Figure 5. Cross-sectional details of BRBs

Table 1 Geometric dimensions and structural properties of BM

Series	Specimen	Type	L	B	t	A(mm^2)	λ	δ_y	Stopper
S-I	FE-4.0			99.8	10.3	1028	457	1.91	Yes
	FT-3.5	SM400A	1375	100.2	10.6	1060	438	1.91	Yes
S-II	FT-4.0(NS)			100.0	10.6	1060	438	1.91	No
	FT-3.5(NS)			100.3	10.2	1026	461	1.91	No

Note: L = length of brace member without cruciform part; B = width; t = thickness; A = sectional area; λ = slenderness ratio on weak axis; δ_y = Nominal axial yield displacement. Unit: mm.

Table 2 Material constants of BMs

Series	Type	E (GPa)	σ_y (Mpa)	ε_y (%)	σ_u (Mpa)	ε_u (%)	ν
S-I	SM400A	210	291	0.139	433	30.2	0.285
S-II		209	251	0.130	409	29.2	0.280

Note: E = Young's modulus; σ_y = yield stress; ε_y =yield strain; σ_u =tensile strength; ν =Poisson ratio.

Table 3 Geometric dimensions and structural properties of RMs

Series	Type	E^R (Gpa)	σ_y^R (Mpa)	b_f (mm)	t_f (mm)	Gap width (mm) d	d_0
S-I	SM400A	198	260	201	14.3	1	2
S-II		212	264	201	14.3	1	2

Note: E^R=Young's modulus; σ_y^R =yield stress; Notations of b_f, t_f, d and d_0 refer to Fig.5.

Table 4 Test results of BRB's specimens

Series	Test specimen	$\Delta\varepsilon/2$	$\Delta\varepsilon$	$\Delta\varepsilon_e$	$\Delta\varepsilon_p$	N_f	CID	Failure position
S-I	FE-4.0	0.040	0.08	0.006	0.074	7	0.96	Mid-span
	FT-3.5	0.035	0.07	0.005	0.065	9	1.18	Mid-span
S-II	FT-4.0(NS)	0.040	0.08	0.006	0.074	4	0.59	Mid-span
	FT-3.5(NS)	0.035	0.07	0.005	0.065	5	0.65	Mid-span

Note: $\Delta\varepsilon/2$ = strain amplitude; $\Delta\varepsilon$ =strain range; $\Delta\varepsilon_e$ = elastic strain range; $\Delta\varepsilon_p$ = plastic strain range; N_f = number of failure cycles; CID = cumulative inelastic deformation.

(2) Test equipment

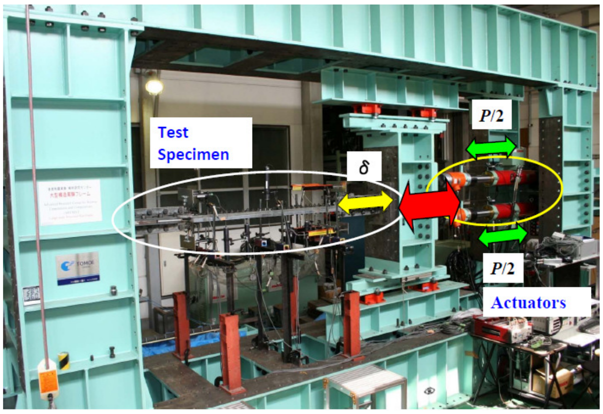

Figure 6. Testing equipment

As shown in Figure 6, the specimen is horizontally pinned by high-strength bolts between two rigid pillars while the BM is horizontally placed. The loading is applied by two jacks parallelly arranged in the vertical direction. The edge of specimens is well treated to avoid eccentric axis load. Before installing specimens, the initial deflection of the specimen is measured in the direction perpendicular to the plate plane so that the initial deflection could direct downward. During a typical experiment, axial displacements of the restrained yielding segment were monitored using eight displacement gauges. These gauges were mounted on both ends of the specimen and displacements were collected by a digital data acquisition system.

(3) Loading pattern

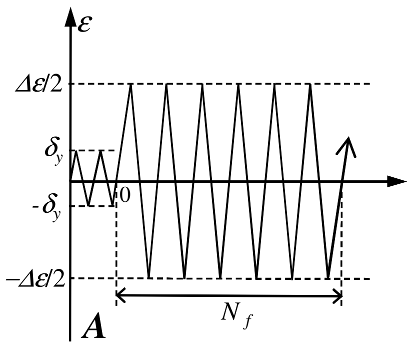

Figure 7. Strain-controlled loading pattern

In the present study, a tensile and compressive alternative cyclic loading controlled by the axial strain of specimens is illustrated in Figure 7. Two cycles of the axial loading of the yield strain amplitude are firstly imposed as an evaluated procedure for testing the specimen and system. For this reason, counting of the cycles starts subsequently. As shown in Figure 7, this constant strain amplitude specified in Table 4 is imposed cyclically until the failure of the BM in the tests. When the loading displacement becomes steady, the strain control equals to the displacement control. Therefore, the present fatigue tests are conducted by controlling the axial displacement. In this experiment, the strain amplitudes of 3.5% and 4% are employed to verify the extreme low-cycle fatigue performance of BRB. Although they are larger than the target axial strain of HPBRB, the following test results show that the specimens possess the excellent performance.

4. TEST RESULTS

(1) Stress-strain curves

The experimental stress-strain curves of the specimens are given in Figure 8. The tensile state of BRBs is displayed in the positive direction. The abscissa is the engineering strain, ε, defined as the relative displacement divided by the original length of both ends of the core plate, while the ordinate is the engineering stress, σ, defined as the axial force divided by the original cross-sectional area of the core plate. The core plate indicates the portion of the BM where it behaves plastically. Test results of all the specimens are summarized in Table 4. In addition, stable stress-strain curves were obtained without overall buckling occurrence in the whole loading history of all the specimens even though the maximum strain amplitude was as large as 4%.

It is shown in the hysteretic curve of the FT-3.5 specimen with the constant strain amplitude that the first loop is hardly affected by the strain hardening effect while the others are remarkably influenced by the strain hardening effect. At the last loop, the strength decreases rapidly in the tensile state of the BM and then unloading is applied when the axial force fells down by over 10% of the maximum axial force. The same results can be observed in other specimens with the constant strain amplitude.

Hysteretic behaviors of BRB's specimens are unsymmetric in tension and compression, and the maximum absolute compressive stress is 21% to 37% larger than the maximum tensile stress. The reason for this behavior is explained as follows: with the strain amplitude increasing in the compressive state, the contact force and the friction between RMs and the BM increased under the multi-wave deformation.

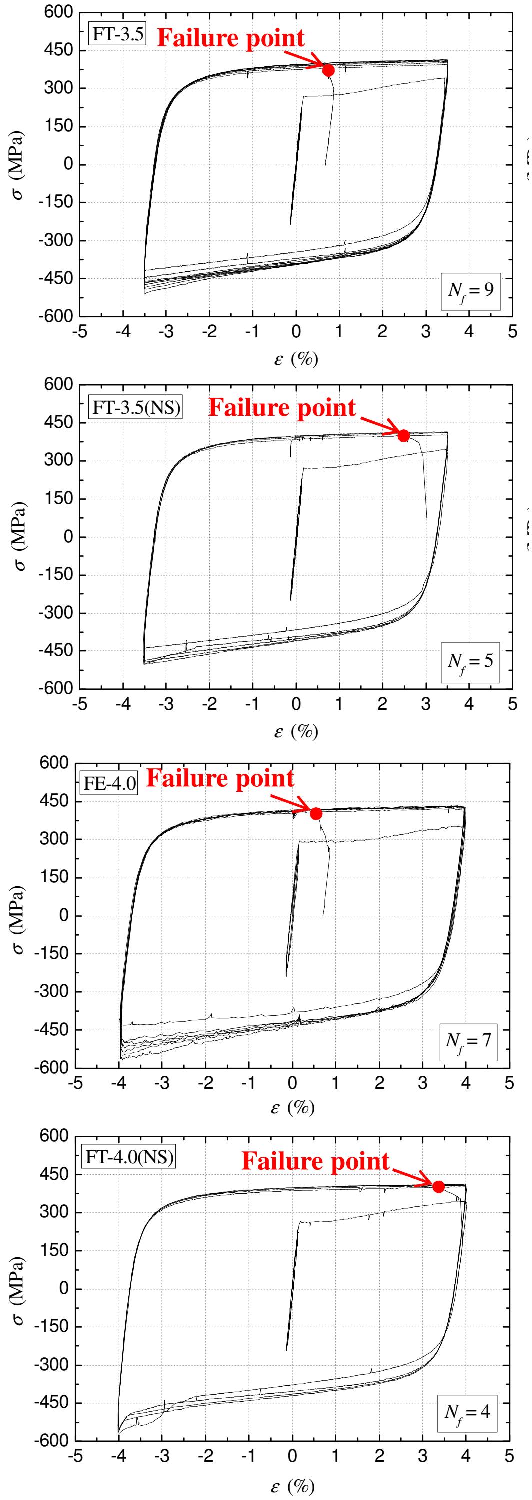

Figure 8. Stress-strain relations

(2) Performance verification

As listed in Table 4, the failure cycle number N_f of the FT-3.5 specimen with the stopper under the same 3.5% strain amplitude decreased from 9 to 5 in contrast with the FT-3.5(NS) specimen without the stopper, while N_f of the FE-4.0 specimen with the stopper under the same 4.0% strain amplitude decreased from 7 to 4 in contrast with the FT-4.0(NS) specimen without the stopper. It can be concluded that the stopper used to prevent the relative displacement obviously affects the low-cycle fatigue performance of steel BRBs.

Failure modes of the BMs are presented in Figure 8, while failure positions of all the test specimens are sketched out in Figure 9(e). It is clear that crack initiating from the mid-span of the BMs induced the failure of specimens. From the failure modes of the FT-3.5 and FE-4.0 specimens with the stoppers, crack began to appear on the side of the BM and propagated in the transversal direction, but from the failure modes of the FT-3.5(NS) and FT-4.0(NS) specimens without the stoppers, crack began to develop in the middle of the BM and the fold deformations were observed after the failure of the BRB's specimens. So, it is concluded that the stoppers have a noticeable impact on the failure of the BRB.

The *CID* values of all test specimens are summarized in Table 4. The calculation of the *CID* was achieved with an algorithm that detects local peaks and valleys in the strain history. *CID* values indicate that the *CID* performance of steel BRBs with the stoppers even under the strain amplitude, larger than 3%, can meet the requirement of high-performance BRBs but *CID* performance of steel BRBs without the stoppers cannot meet the requirement of high-performance BRBs.

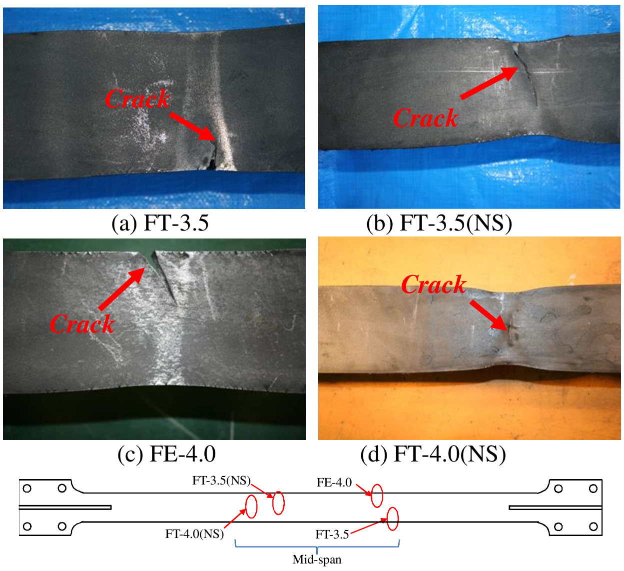

(a) FT-3.5 (b) FT-3.5(NS)
(c) FE-4.0 (d) FT-4.0(NS)
(e) Failure position

Figure 9. Failure modes of BRB's specimens

5. CONCLUSIONS

In this study, extreme low-cycle fatigue tests of BRBs with or without the stoppers were carried out to evaluate the effect of stoppers on the low-cycle fatigue performance or the performance of the proposed HPBRB. The main results are summarized as follows:

1) Extreme low-cycle fatigue tests were conducted to verify that the BRB's specimens with the stoppers possess the better low-cycle fatigue performance and the larger safety margin than the specimens without the stoppers.

2) It was experimentally confirmed that the *CID* performance of steel BRBs without stoppers decreased by 45% and 39% compared to BRBs with stoppers under the 3.5% and 4% strain amplitudes, respectively.

ACKNOWLEDGMENT: This research was performed under Grants from the Advanced Research Center for Seismic Experiment and Computations (ARCSEC), Meijo University.

REFERENCES

1) Usami T, Lu Z, Ge H. *A seismic upgrading method for steel arch bridges using buckling-restrained braces*, Earthquake Engineering & Structural Dynamics, 34 (4-5): 471-496. 2005.

2) Usami T, Ge HB, Kasai A. *Overall buckling prevention condition of buckling-restrained braces as a structural control damper*. 14th World Conference on Earthquake Engineering, Beijing, China, 2008.

3) AISC. *Seismic provisions for structural steel buildings*, Chicago, Illinois, 2005.

4) Usami T. *Developing high-performance damage control seismic dampers*. 10th symposium on ductile design method for bridges (Special Lecture), 2007(in Japanese).

5) JSCE. *Standard specifications for steel and composite structures-2008, IV seismic design*, 2008(in Japanese).

6) Usami T, Sato T. *Low-cycle fatigue tests and verification method for a steel buckling-restrained brace*, Journal of Structural Engineering, JSCE, 56A: 486-498. 2010 (in Japanese).

7) Usami T, Wang C-L, Funayama J. *Low-cycle fatigue tests of a type of buckling restrained braces*. 12th East Asia-Pacific Conference on Structural Engineering and Construction, Hongkong, 2011.